SLAC-PUB-10175
September 2003

Effect of RF Parameters on Breakdown Limits in High-Vacuum X-Band Structures*

Valery A. Dolgashev and Sami G. Tantawi

Stanford Linear Accelerator Center, Stanford University, Stanford, CA 94309

Abstract

RF breakdown is one of the major factors determining performance of high power rf components and rf sources. RF breakdown limits working power and produces irreversible surface damage. The breakdown limit depends on the rf circuit, structure geometry, and rf frequency. It is also a function of the input power, pulse width, and surface electric and magnetic fields. In this paper we discuss multi-megawatt operation of X-band rf structures at pulse width on the order of one microsecond. These structures are used in rf systems of high gradient accelerators. Recent experiments at Stanford Linear Accelerator Center (SLAC) have explored the functional dependence of breakdown limit on input power and pulse width. The experimental data covered accelerating structures and waveguides. Another breakdown limit of accelerating structures was associated with high magnetic fields found in waveguide-to-structure couplers. To understand and quantify these limits we simulated 3D structures with the electrodynamics code Ansoft HFSS and the Particle-In-Cell code MAGIC3D. Results of these simulations together with experimental data will be discussed in this paper.

Paper presented at the RF 2003 Workshop
Berkeley Springs, West Virginia, USA June 22-26, 2003

*Work supported by the U.S. Department of Energy contract DE-AC03-76SF00515.

Effect of RF Parameters on Breakdown Limits in High-Vacuum X-Band Structures

Valery A. Dolgashev and Sami G. Tantawi

SLAC, Stanford, CA 94025, USA

Abstract. RF breakdown is one of the major factors determining performance of high power rf components and rf sources. RF breakdown limits working power and produces irreversible surface damage. The breakdown limit depends on the rf circuit, structure geometry, and rf frequency. It is also a function of the input power, pulse width, and surface electric and magnetic fields. In this paper we discuss multi-megawatt operation of X-band rf structures at pulse width on the order of one microsecond. These structures are used in rf systems of high gradient accelerators. Recent experiments at Stanford Linear Accelerator Center (SLAC) have explored the functional dependence of breakdown limit on input power and pulse width. The experimental data covered accelerating structures and waveguides. Another breakdown limit of accelerating structures was associated with high magnetic fields found in waveguide-to-structure couplers. To understand and quantify these limits we simulated 3D structures with the electrodynamics code Ansoft HFSS and the Particle-In-Cell code MAGIC3D. Results of these simulations together with experimental data will be discussed in this paper.

INTRODUCTION

Accelerating gradient is one of the crucial parameters affecting the design, construction and cost of next-generation linear accelerators. For a specified final energy, the gradient sets the accelerator length, and for a given accelerating structure and pulse repetition rate, it determines power consumption. The present Next Linear Collider (NLC) and Japanese Linear Collider (JLC) design specifies accelerating gradient of 65 MV/m at 11.4 GHz [1], this is almost 3 times larger than the present operating gradient of S-band SLAC linac.

Among phenomena that limit the gradient is rf breakdown in accelerating structures, rf sources and waveguide components.

This paper discusses experimental results and problems related to breakdown damage, pulsed heating, and gradient limitation due to input rf power in waveguides and accelerating structures.

History

Due to limited available rf power, early high gradient experiments were done with standing wave (SW) structures and short low group velocity traveling wave (TW) structures. The highest gradient obtained during the SLAC construction period (1962-1966) is mentioned in [2]. This gradient was obtained with a short accelerating structure in a resonant ring. It is believed that this structure reached an accelerating gradient of 46 MV/m without obvious signs of breakdown. The surface gradient for this structure was about

two times larger than the accelerating gradient. Early high gradient research for a linear collider project was published in Novosibirsk in 1978 [3]. A single S-band cavity was tested up to 150 MV/m (2 μs pulse lenght) surface gradient. This gradient was limited not by breakdowns but by field-emission currents. Standing wave structures were tested at different frequencies with reported surface gradient of 340 MV/m (2.5μs, S-band), and 572 MV/m (0.77μs, X-band) [2].

For the TW structures the surface gradient was somewhat lower: 285 MV/m (0.15 μs, X-band) [4]. This gradient was achieved in the first cell of a constant impedance structure. Similar results were obtained during *backward* processing of the DS2 structure [5]. There, rf power was fed into an output coupler of this close-to-constant gradient structure and the maximum surface electric field was in the output coupler cell. These structures were mostly built specifically for high gradient tests. The testing procedure also was focused on maximum achievable gradient. Structure damage, breakdown rate (number of pulses with breakdowns per hour) or heavy loading by dark current were not addressed.

Operational Gradients

Operational gradients with a low fault rate are lower than the maximum obtained gradient. An operational gradient of 40 MV/m was reported for a 1.5 meter constant impedance TW S-band structure for the Stanford Linear Collider positron injector. This corresponds to a maximum surface field of 80 MV/m [6]. A typical operational gradient for SW S-band structures of a medical linear accelerator is 30 MV/m, with surface electric fields of 130 MV/m [7] at a pulse width of several microseconds (longer than the working pulse width for SLAC TW structures). SW structures for S-band rf guns routinely operate at maximum surface fields of 130 MV/m ($\sim$2 μs pulse width) [8]. We note that operational surface fields in the above discussed SW structures are higher than that in TW structures.

With the development of more powerful rf sources, operational tests of several prototypes of NLC/JLC 1.8 m TW X-band structures started in the late 1990s. Some of them have shown damage at input power levels around 90 MW and average gradient of 50 MV/m (250 ns) [9]. As a consequence, extensive experimental and theoretical programs to resolve the problems of high gradient operation of the accelerating structures were started in SLAC, KEK and CERN. These programs included testing TW and SW accelerating structures, waveguides, and single cavities.

In this paper we will refer to recent experimental results on TW structures [1], SW structures [10] and waveguides [11]. The parameters where the breakdown phenomena was systematically tested are close to the NLC parameters. The frequency is 11.424 GHz, rf power up to 150 MW, pulse length up to 400 ns for SW and TW accelerating structures and up to 1.5 μs for waveguides.

RF BREAKDOWN

RF breakdown is a major factor determining the practical operating gradient of an accelerating structure. It leads to disruption of operation and damage to the surface. Characteristics of rf breakdown and multiple theories of breakdown physics can be found in bibliographies of two Ph.D. dissertations [2, 12]. The scope of this paper will be limited to those properties of rf breakdown that effect design and operation of high power rf components. These properties are the breakdown rate and the damage induced by the breakdowns. These parameters are not independent. We conjecture that the damage is more related to power absorbed during a breakdown event, while the breakdown rate is determined by the amplitudes of surface electric and magnetic fields, geometry, metal surface preparation and conditioning history. The conditioning history is in turn effected by the breakdown induced damage.

General Properties of a Breakdown Event

RF breakdown is a phenomenon that abruptly and significantly changes transmission and reflection of the rf power directed toward the structure under test. Breakdown is accompanied by a burst of x-rays and by a bright flash of visible light. Listed here are some properties of the rf breakdown in TW structures and waveguides [13]:

1. During breakdown the transmitted power drops to unmeasurable levels with time constant of the power shut-off of 20–200 ns.
2. Up to 80% of the incident rf power is absorbed by the arc.
3. In waveguide experiments, spectral lines of the light emitted from the breakdown site are mostly from neutral copper atoms [11].

With respect to the rf energy absorbed in the breakdown, the behavior of SW structures is very different from TW structures [13]. In TW structures during most breakdowns, a large fraction of the incident energy is absorbed by the breakdown. In SW structures during most breakdowns, most of the rf power is reflected from the structure. After breakdown starts, reflected power increases during about 100 ns in the TW structure breakdowns, and in about 10 ns in most SW breakdowns. Not all breakdowns in the SW structures have this character, some breakdowns do not produce large reflection.

Simulations

3D and 2D Particle-In-Cell simulations of the breakdown dynamics give a possible explanation of the breakdown development [13]. The simulation was based on a model of a “plasma spot”[14]. We assume that at some moment after structure is filled with rf energy a plasma spot appears on the structure surface. The physics of the event that triggers the plasma spot in rf structures remains unknown. The plasma spot is simulated by the creation of an emission area in the structure (spot size 2 mm^2...100 mm^2). Space-charge limited emission of electrons from the spot was used. A beam of copper ions was

generated in the same area with a predetermined current density. The main results of these simulations for TW structures and waveguides are:

1. The major energy exchange between incident rf fields and particles comes from the interaction of the rf electric fields with electrons (not with ions). Electrons cross the gap in the waveguide or accelerating structure cell in a short time (about an rf period).
2. The electron current must be several kA to significantly effect the rf power transmission. Space charge-limited emission of electrons without ions cannot produce and sustain the required current densities.
3. Ion currents of 10–100 A are needed to allow sufficient electron currents to disrupt transmitted power. The space charge field of the ions compensates the electron space charge field. This compensation allows the generation of kA of electron current. The time constant for the drop off of transmitted power is 10–20 ns and is related mostly to the process of filling the waveguide gap or accelerating structure cell with copper ions.
4. Without electrons, the ions do not move significantly during the rf pulse. In the presence of the space-charge limited electron flow, the ion beam crosses the waveguide in about 30 ns and fills the accelerating structure cell or waveguide gap in 20 ns at 60...80 MW of input power. The oscillating space charge field of the electrons adds a DC component to the rf electric field. This DC component accelerates the ions.
5. A significant portion (50–80%) of the emitted electrons and ions returns to the emitting spot and the surrounding area. We note that in the simulations relatively large spot size (from 2 mm^2) was used. The smallest spot size is determined by the minimal mesh size of the PIC code.
6. Up to 50% of the input power can be absorbed by the ion-electron beam in the waveguide and up to 60% in TW accelerating structure. To explain the absorption of an additional 20% the model requires the introduction of some effects associated with the interaction of electrons with neutral copper atoms and possible expansion of the emission spot.

RF Conditioning

The breakdown rate and the gradient limit for TW structures, SW structures and waveguides behave similarly with change of input rf parameters:

1. The breakdown rate changes over time. While the structure accumulates breakdowns from the start of conditioning, the rate drops for constant input power and pulse width. Usually during processing the breakdown rate is kept roughly constant while input power and pulse width are increased until the desired value or the gradient limit is reached. Here we define the limit as a gradient where breakdown rate no longer decreases with accumulated breakdowns. In some cases we saw degradation of a structure performance — the breakdown rate begins to slowly increase after reaching the limit of initial processing.

2. The number of breakdowns required to reach the limiting gradient varies greatly (sometimes by factors of 10) with the preparation of the structure surface. The source of this difference is not understood, and is being intensively studied. At the same time the limiting gradient for TW structures depends weakly on the surface preparation. Typical variation of final gradient for the same structure geometry and same breakdown rate is within 10–20%.
3. At each stage of processing the breakdown rate increases with increasing power and pulse width. The behaviour of the "constant-breakdown rate curve" usually could be fitted with function Pt^{α}. Here P is input power, t – pulse length, and $\alpha \sim 0.3...0.5$.
4. The breakdown rate grows almost exponentially with the power [10, 1]. On a linear scale, it appears like the breakdown rate has a threshold.
5. Variation of vacuum pressures below 10^{-7} Torr does not seem to effect breakdown rate.
6. The amplitude of the dark current emitted from the structures and waveguides follow Fowler-Nordheim dependence on the surface electric fields fitted with field amplification factor β. For X-band TW structures $\beta = 30...40$. This value of β is similar and reproducible for different TW accelerating structures.
7. Without breakdowns the amplitude of dark currents does not depend on pulse length. Each breakdown in waveguides can change the amplitude of the dark current by 10–300%. In accelerating structures each breakdown does not significantly change the dark current. We emphasize the difference between the breakdown currents and the dark currents.
8. The metal surface of the structure is obviously modified during rf processing in a way that it could sustain gradients higher than the gradients at start of rf processing. Physics of these processes is still unknown. Observable parameters such as surface roughness are significantly worse (with craters and metal droplets) after processing compared to carefully prepared surfaces before processing.

The breakdown behaviour and the processing behaviour of TW structures and waveguides are very similar, even though the peak amplitudes of surface electric fields are very different. The surface field at the gradient limit for waveguides is significantly lower than in accelerating structures (for the same pulse width). For example, at 400 ns pulse length, low-magnetic-field waveguide had surface gradient of about 80 MV/m [11] while highest surface field in the TW53VG3MC TW structure [1] was about 200 MV/m. For high-magnetic-field waveguide this field was even lower at about 60 MV/m. We conjecture that the source of this difference is the effect of surface damage on the gradient limit and this phenomena will be discussed below.

During processing the structure accumulates a certain number of breakdowns before reaching the gradient limit. For recently tested TW structures and SW structures [1, 10] this number breakdowns is usually below 10^4. Since the gradient limit for structures of the same geometry is weakly dependent on the initial condition of the structure it is possible that this limit is determined by the geometry and the properties of the metal. Below we will discuss two possible phenomena that prevent structures from further conditioning. These phenomena are determined by the structure geometry and

the properties of copper: rf breakdowns due to combination of high rf magnetic fields (1 MA/m for 400 ns pulse length) with moderate electric fields (100 kV/cm), and limits due to metal surface damage.

BREAKDOWN AND RF MAGNETIC FIELDS

Low group velocity TW structures and SW structures were high-power tested [18]. The maximum gradient in all of these structures was limited by breakdowns in couplers. The damage was concentrated in input couplers [19]. In earlier experiments, the breakdowns were frequently observed in coupler cells of accelerating structures and have been attributed to the electrical field enhancement noted in simulations. Several solutions have been proposed to reduce this enhancement [20, 21]. For example, increasing the group velocity in the coupler and adjacent cells, and shaping of the coupler cell to reduce maximum surface electric fields below the fields in the structure. Less attention was paid to enhancement of the magnetic field in the couplers although the possibility of copper surface damage due to pulse heating was suggested in [22].

The limit imposed on operational parameters of accelerating structures by rf pulse heating and thermal fatigue was discussed in [23, 24], but the connection between the high rf magnetic field and coupler breakdowns was only realized in the above mentioned experiments [25, 26, 10].

Experimental Results

There is overwhelming experimental evidence that the waveguide-to-coupler irises in couplers are prone to breakdowns in low group velocity TW structures and in SW structures.

The breakdowns produce mechanical shock. Shock waves were registered by acoustic sensors installed on the input coupler of a TW structure. The data have shown that the location of the source of the acoustic signal is correlated to the location of waveguide-to-coupler-cell irises [15].

A video-camera was used to obtain images of the arcs in the SW structures. Averaging of more than 100 images again shows that the visible arc location corresponds with the location of the waveguide-to-coupler-cell irises [10].

An autopsy of a TW structure has shown that the inner edges (cell side) of the waveguide-to-coupler-cell irises are eroded while the outer edges (waveguide side) are almost undamaged. The damage was roughly uniform over the height of the irises as seeing in Fig. 1 [16].

Detailed electrodynamic simulation of the TW and SW structure couplers was made in order to understand the physics underling coupler breakdowns. For the simulations the commercial frequency-domain code Ansoft HFSS^{TM}[17] was used. The simulations are discussed in [27]. Here we provide main results of that work.

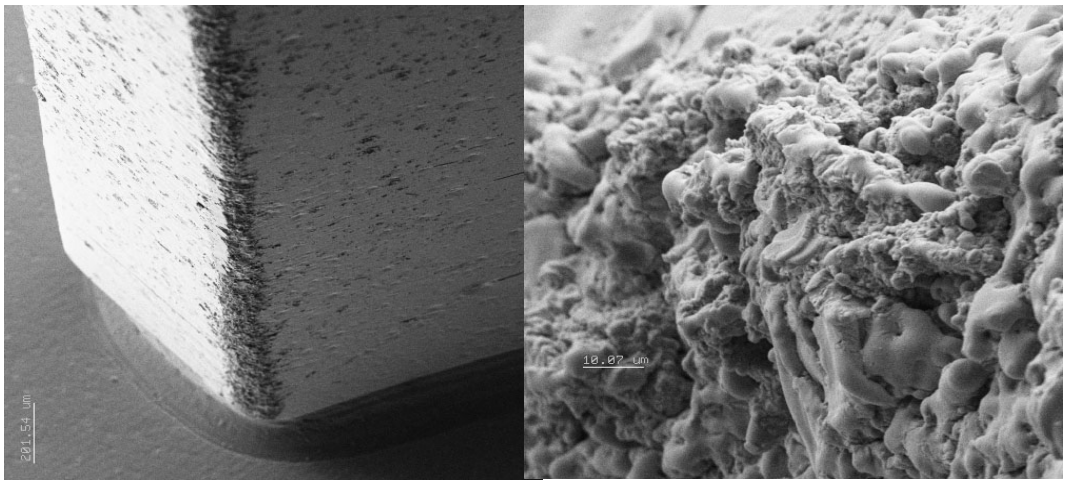

FIGURE 1. SEM image of inner edges (cell side) of the waveguide-to-coupler-cell irises.

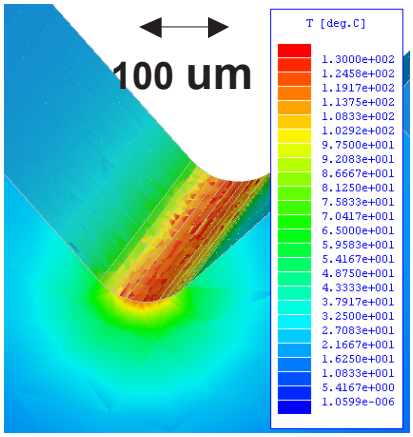

FIGURE 2. Temperature distribution on the inner edge of the waveguide-to-coupler-cell iris (maximum current 0.7 MA/m, 400 ns).

Magnetic Fields on Sharp Edges of Waveguide-to-Coupler Irises

RF power enters the structure through the opening made by two waveguide-to-coupler irises. The rf surface currents flow along the edges of each iris. This edge is a place where local rf currents are significantly amplified. The radius of the waveguide-to-coupler cell iris edge was specified on the drawing at $76 \pm 25 \mu$m. Thickness of the iris (distance between edges) is 0.8 mm. Simulations produce for 76 μm rounding approximately 2.5 times magnetic field enhancement on the corner compared to the field between edges. The metal on the edge is heated by the rf currents. The RF heating of a metal surface was calculated with a 1D model using calculated tangential magnetic field $H_{||}$ [24]. The maximum pulse temperature rise ΔT is given by :

$$\Delta T = \frac{|H_{||}|^2\sqrt{t}}{\sigma\delta\sqrt{\pi\rho' c_\varepsilon k}},$$

where σ is the electrical conductivity, δ is the skin depth, ρ' is the density, c_ε is the specific heat, and k is the thermal conductivity of the metal. For copper at a frequency of 11.424 GHz the temperature rise $\Delta T = 430|H_{||}|^2\sqrt{t}$, where ΔT is in °C, $H_{||}$ in MA/m, and t is in μs. In this simplified model, nonlinearities of the metal's physical properties are neglected. Since we are using this simplified model, we treat the calculated pulse temperature rise more like a parameter that characterizes the geometry of the structure than the real temperature of the metal surface. Calculation of the real pulse temperature rise might be difficult because the properties of the metal change with evolving surface damage [24]. Other unknowns are metal thermal and electrical conductivities at the pulse currents of order of megaampere per meter and pulse length of hundreds of nanoseconds [29].

Some of the couplers were cut open after the test. Damage to edges observed on the microscope images was correlated with calculated pulse temperature rise of about 100°C. The calculated pulse temperature rise for iris shown in Fig. 1 is shown in Fig. 2.

But predicting the breakdown behavior using the calculated pulse temperature rise was difficult. All structures have shown threshold-like breakdown behavior with the input rf power and pulse width similar to that given in [10]. The calculated pulse temperature rise correlating to the threshold varied between 60 to 150°C, but not all couplers with similar rf magnetic fields where breaking down. This observation suggested that pulsed heating by itself is not enough to cause the breakdowns and prompted a closer look at the surface electric field.

Edge Electric Fields

This edge surface electric field is commonly ignored since it has much lower amplitude than the maximum field in the cell. A real structure with irises and beam pipes always has electric field on the outside diameter of the cell (compared to the idealized case of a pill-box cavity with TM010 mode). While th sharp edge on the waveguide-to-coupler iris enhance this field.

Input and output couplers of a 60 cm structure with initial $v_g = 0.03c$ were simulated using HFSS. The coupler irises were modeled with 80 μm rounding. The surface electric field distribution on the iris edges is shown in Fig. 4. For unloaded gradient of 70 MV/m the input coupler has 13 MV/m maximum field on the edge. The output couplers have about 2 MV/m on the iris edge. The calculated pulse temperature rises are 270° and 160°C respectively. During the high power test the input coupler was breaking down, but the output coupler did not.

The importance of the edge electric field was supported by following data. A coupler that had more than 150°C calculated temperature rise but no breakdowns was autopsied. It had damage on the iris edges. The damage was roughly uniform along the height of the iris but looked very different from damage in couplers with breakdowns (see Fig. 3) [28].

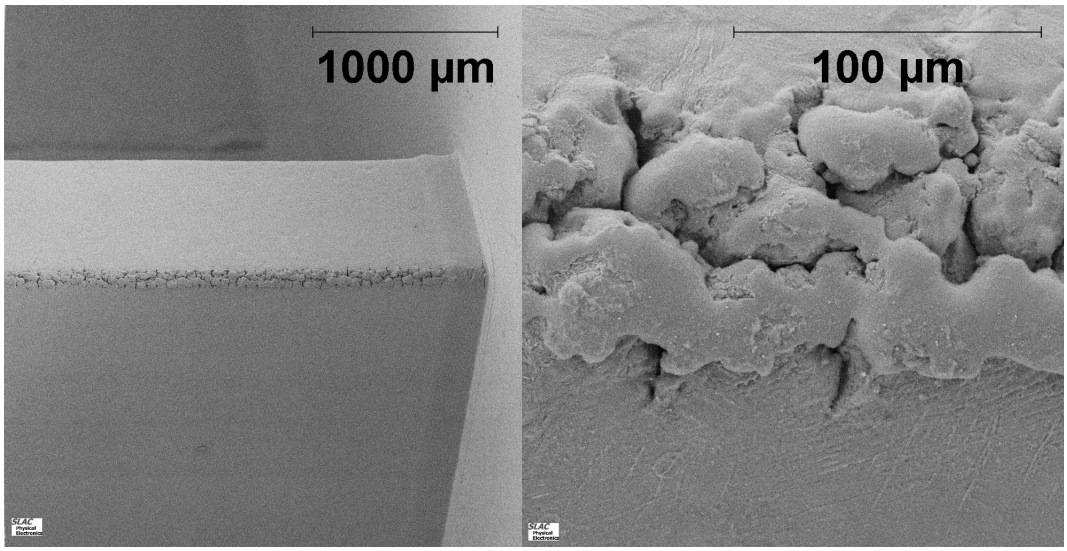

FIGURE 3. SEM image of inner edges (cell side) of the waveguide-to-coupler-cell irises of the coupler that had no breakdowns. The calculated pulse temperature rise on the edge of the iris is above 180 °.

The calculated electric field on the edge of the waveguide-to-coupler-iris was about 1 MV/m. This data give a possible range of electric fields required for the breakdown trigger in combination with high magnetic fields (that produce pulse temperature rise of about 100°): electric fields on the order of 10 MV/m are needed to start breakdown, while fields of about 1 MV/m are probably safe.

Breakdown Trigger

The damage observed on the coupler edges and the breakdown behaviour suggests that the breakdown trigger is related to *mechanical fatigue* of the copper surface. In the the model described in [30] the mechanical fatigue accumulates with each pulse and after certain number of pulses a macroscopic change occurs (similar to creation of a dislocation). This model needs an additional assumption, which is, that this macroscopic change triggers the rf breakdown. It seems that the moderate electric fields ($\sim$ 10 MV/m) on the edges are an essential part of this trigger. The physics of the surface heating also needs verification since other effects like single surface multipactor discharge in strong rf magnetic fields could increase the surface temperature in addition to the Joule heating from rf currents.

New Low Surface Magnetic-Field Couplers

After the source of coupler breakdowns was traced to high magnetic fields on the sharp edges of the waveguide-to-coupler cell irises, an obvious solution followed: increase the iris rounding to reduce magnetic surface fields. To determine the sufficient

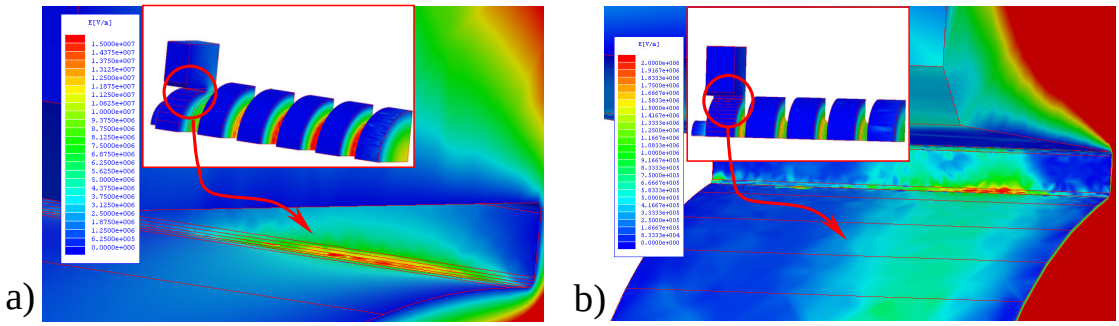

FIGURE 4. Surface electric field distribution on the edge of 60 cm, $v_g = 0.03c$ structure: a) input coupler, maximum edge field ∼13 MV/m; b) output coupler, maximum edge field ∼2 MV/m.

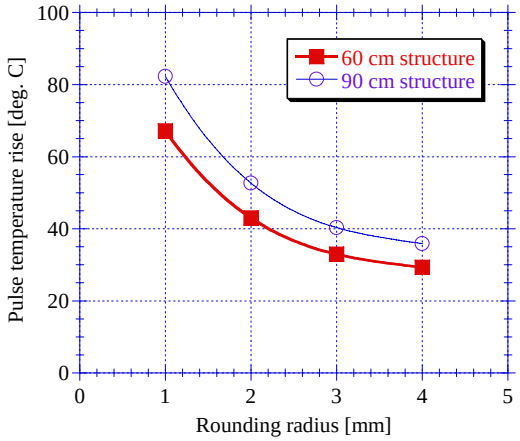

FIGURE 5. Dependence of maximum pulse temperature rise *vs.* waveguide-to-coupler iris rounding for 60 cm and 90 cm long accelerating structures. Points — simulation, curves — polynomial fit.

rounding an NLC prototype structure was matched by couplers with different iris rounding. That structure is 60 cm long, constant gradient, with initial group velocity (v_g) of 3% of speed of light (c) and 150° phase advance per cell. Several couplers with different rounding were matched. Results of the calculation for 60 cm and 90 cm long structures with the same input coupler, 70 MV/m unloaded gradient, pulse width of 400 ns, are shown in Fig. 5. The shorter structure needs 70 MW of input power while the longer one needs 96 MW to reach this gradient. The temperature rise for the 90 cm, $v_g = 0.03c$ structure has been scaled up from the 60 cm structure results as both structures have the identical input couplers. Iris rounding of 3 mm was chosen for the new couplers in order to keep the pulse temperature rise way below 100° C. Couplers for several structures with such rounding were designed, built and successfully tested at high power. Example of such coupler is shown on Fig. 6a. Performance of these structures was not limited by coupler breakdowns [1]. At the same time, new coupler designs have been developed to considerably decrease the pulse temperature rise and the surface electric field [31]. An example of a low surface magnetic-field coupler of waveguide type is shown on Fig. 6b.

a) 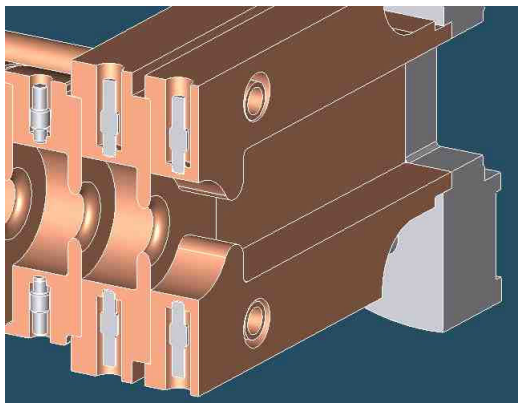 b) 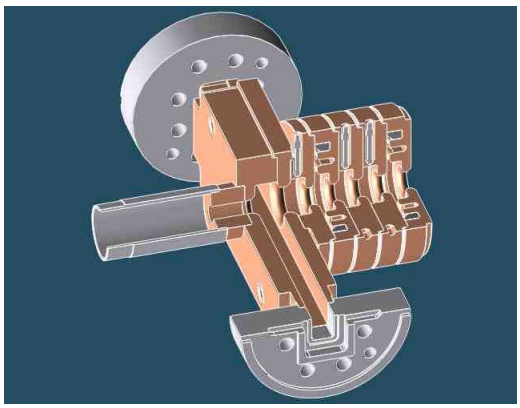

FIGURE 6. Cut-away view of two low-magnetic field couplers: a) fat-lipped coupler; b) waveguide coupler.

BREAKDOWN LIMITS DUE TO INPUT POWER

There is a possibility that one of the phenomena that limits the operational gradient in TW structures and waveguides is the breakdown damage of the copper surface during rf conditioning. We note that this phenomena was studied in NLC parameters of rf power below 150 MW, pulse length below 400 ns for the TW structures and <1.6 μs for waveguides and surface electric fields <240 MV/m for TW structures and <100 MV/m for waveguides. Other then for these parameters and for different structures, for example for SW structures, the limiting phenomena might be different.

We emphasize the difference between the operational gradient for low fault rate compared to maximum achievable gradient. To illustrate this difference we can use data from recent processing of TW structures at SLAC [1]. In Fig. 1 of [1] is shown a typical dependence of breakdown rate (breakdowns/hour) *vs.* average gradient after the structure was processed close to the gradient limit. For repetition rate of 60 Hz the slope of the function is about $1/(8\ \text{MV/m})$ per decade of breakdown rate. Obviously, for short time the structure could reach much higher gradient than the operational gradient (at breakdown rate of one per 10 hours). We note that this particular structure had modified couplers with 3 cm rounding of the waveguide-to-coupler irises and did not have breakdowns in couplers.

Breakdown behaviour during initial processing is different from breakdown behaviour at the gradient limit. Below we will discuss the structure behaviour *at the gradient limit* and at the relatively small breakdown rate < 10/hour at 60 Hz, since this gradient limit and the breakdown behaviour is reproducible for different TW structures with similar geometries.

There are several experimental observations that suggest that the breakdown induced surface damage and the gradient limit in TW structures are related:

1. Near the gradient limit most breakdowns and damage in TW structures are concentrated in the beginning of the structure where incident power (and group velocity) is highest. For example, measurements of the 1.8 m TW prototypes have shown

that the input part of the structures is damaged [32, 9]. The output part of these structures had lower local rf power and lower group velocity (5%–2%*c*) and the damage was barely measurable.

2. TW structures that require less power to reach the same gradient (with higher shunt impedance) have reached higher gradients than the structures with lower shunt impedance. The power at limiting gradient was about 90 MW (400 ns pulse length) and it is roughly independent of structure type. For example, the high shunt impedance structure T53VG3MC have reached 90 MV/m, and low shunt impedance H90VG3 have reached only 65 MV/m at similar breakdown rate of <0.1/hour, and similar power of about 90 MW [1].
3. When a TW structure or waveguide is run with power and pulse length close to the limiting gradient, its breakdown behaviour significantly changes. “Breakdown chains” appear: after an initial breakdown, several more cluster close to each other in location and time. In many cases secondary breakdowns follow after the initial breakdown at much lower power and pulse length during after-breakdown procedure of ramp up of power and pulse lenght.

There is a qualitative change of the breakdown behaviour near the gradient limit such as concentration of breakdown locations and damage at the beginning of the structure and appearance of “breakdown chains”. This change in breakdown behaviour suggests that there exists some kind of threshold combination of rf power and pulse length that sharply increases damage induced by breakdowns. We conjecture that this increased damage is preventing the structure from conditioning to higher gradients. This assumption contradicts the hypothesis that the gradient limit is determined by microscopic parameters such as peak surface electric field and surface cleanliness and roughness, since the value of input power at the gradient limit was quite reproducible and weakly depended on values of peak surface electric fields and on initial surface preparation.

The assumption that this threshold is related directly to the amount of energy absorbed in breakdowns (the absorbed energy routinely measured in experiments) contradicts well established scaling of the breakdown rate with rf power and pulse width Pt^{α}. We conjecture that physics behind power related gradient limit in TW structures might be similar to physics of phenomena observed in high current DC arcs. A similar conjecture was used in [33].

DC Experiments on Relation of Gradient Limit and Arc Energy

A study of degradation of high voltage performance of the copper electrodes in vacuum with arc current >5 kA was published in [34]. The author suggests that the degradation is due to abundance of molten debris.

Systematic study of dependence of the DC gradient limit on energy available for the arc was done at Novosibirsk during development of gridded X-band klystron [35]. The author changed the size of capacitors feeding arc and then studied the processing curves (hold-off voltage *vs.* consequent breakdown number). This curves were different for different size of capacitor: below a certain value of capacitor the hold-off voltage was

increasing with consequent breakdowns; above it has shown "chain breakdowns" and with further increase of capacitance the hold-off voltage decreased.

The authors of [36, 37] have systematically studied electrode erosion in high-current, high-energy transient arcs. They found that if the value of $P'\sqrt{t'}$ for copper electrodes was above a certain threshold value, the amount or material removed from the copper electrodes increased by two orders of magnitude. Here P' is power absorbed by the arc currents and t' is the arc duration. The authors explain this abrupt increase in electrode erosion by ablation of the metal: metal was heated by the arc currents, the temperature of the surface increased proportionally to $P'\sqrt{t'}$ effected by diffusion of the heat into the metal, after melting, the material was removed by ablation.

SUMMARY AND DISCUSSION

In this paper we have discussed two possible phenomena that limit the operating gradient in accelerating structures and waveguides: limits due to combination of high magnetic fields and moderate electric fields, and limit due to input-power-related surface damage. Due to reproducibility of the value of the gradient limits for structures of similar geometries, we conjecture that these limits are based on bulk properties of the metal and on structure geometry and loosely on the properties of the breakdown trigger.

We note that most of the study was done with the NLC parameters (frequency, rf power and pulse widths) and for TW structures. It is possible that other phenomena will limit the gradient outside this parameters. For example, limits due to loading of rf power by field emission (dark) currents. This problem was noted in the early experiments [3]. The power $\tilde{P}$ absorbed by dark current is a very strong function of the surface fields E_s: $\tilde{P} \sim E_s^{\varepsilon}$, where ε ranges from 9 to 20. Due to such strong field dependence of absorbed power this limit should have weak pulse length dependence. Since, in recent tests of the SW and TW structures, dark-current-loading was not observed for surface electric fields up to 200 MV/m, the gradient limited by this phenomena is likely above this level.

Copper structures of two geometries were systematically studied: mostly disk-loaded waveguides (accelerating structures) and rectangular waveguides. We expect that both above mentioned limits are geometry dependent, and the input-power-limit is, obviously, circuit dependent. Examples of other circuits are SW structures [10] or TW structures as part of resonant rings [38]. The amount of energy absorbed during breakdown events in such structures is usually much lower than in TW structures and in waveguides for similar drive power and pulse length.

ACKNOWLEDGMENTS

Work supported by the U.S. Department of Energy contract DE-AC03-76SF00515. Authors appreciate useful discussions and suggestions of Chris Adolphsen and Perry Wilson of SLAC.

REFERENCES

1. C. Adolphsen, "Normal Conducting RF Structure Test Facilities and Results," ROPC006, PAC03, Portland, Oregon, May 12-16, 2003.
2. J.W. Wang, "RF Properties of Periodic Accelerating Structures for Linear Colliders," SLAC-Report-339, Ph.D. Dissertation, Stanford University, 1989.
3. V.E. Balakin *et al*, "Accelerating Structure of a Colliding Linear Electron-Positron Beam (VLEPP), Investigation of the Maximum Attainable Acceleration Rate," Novosibirsk, Nov., 1978, SLAC-TRANS-0187.
4. J.W. Wang *et al*, "SLAC/CERN High Gradient Tests of an X-Band Accelerating Section," CERN-SL-95-27-RF, PAC95 , Dallas, TX, May 1-5, 1995.
5. R. Loewen, "ASTA Structure Operation Results," Presented at Structure Breakdown Workshop, SLAC, August 28 - 30 , 2000.
6. J. E. Clendenin *et al.*, "The High Gradient S-Band Linac For Initial Acceleration Of The SLC Intense Positron Bunch," *Part. Accel.* **30**, 85 (1990).
7. C. J. Karzmark *et al. Medical Electron Accelerators*, McGraw-Hill, Inc., New York, 1993.
8. D. T. Palmer *et al.*, "Emittance studies of the BNL/SLAC/UCLA 1.6 cell photocathode rf gun," SLAC-PUB-7422.
9. C. Adolphsen *et al*, "RF Processing of X-Band Accelerator Structures at the NLCTA," LINAC2000, August, 2000, Monterey, CA.
10. V. A. Dolgashev *et al*, "Status of X-band Standing Wave Structure Studies at SLAC," TPAB031, PAC03, Portland, Oregon, May 12-16, 2003.
11. V.A. Dolgashev, S.G. Tantawi, "RF Breakdown in X-band Waveguides," TUPLE098, EPAC'02, 3-7 June, 2002, Paris, France, pp. 2139-2141.
12. L. Laurent, "High Gradient RF Breakdown Studies," Ph.D. Dissertation, UC Davis, 2002.
13. V.A. Dolgashev, S.G. Tantawi, "Simulations of Currents in X-band accelerator structures using 2D and 3D particle-in-cell code," FPAH057, PAC 2001, June 18-22, Chicago, Illinois. pp. 3807-3809.
14. P.B. Wilson, "A Plasma Model for RF Breakdown in Accelerator Structures," LINAC 2000, Monterey, CA, August, 2000.
15. J. Frisch *et al.*, "Studies of Breakdown in High Gradient X-band Accelerator Structures Using Acoustic Emission," TH484, LINAC02, Gyeongju, Korea, 2002.
16. F. Le Pimpec *et al.*, "Autopsy on an RF-Processed X-band Traveling Wave Structure," MO486, LINAC02, Gyeongju, Korea, 2002.
17. http://www.ansoft.com/products/hf/hfss/
18. "NLC Newsletter," July, 2002.
19. C. Adolphsen *et al.* , "Processing Studies of X-Band Accelerator Structures at the NLCTA," ROAA003, PAC01, Chicago, IL, 2001.
20. N. M. Kroll *et al.*, "Application of Time Domain Simulation to Coupler Design for Periodic Structures," LINAC 2000, Monterey, CA, August, 2000.
21. J. Haimson *et al.*, AAC96, AIP Conf. Proc. 398, p. 898 (1997).
22. O. A. Nezhevenko *et al.*, "34.3 GHz Accelerating structure for High Gradient Tests," PAC01, Chicago, IL, 2001, p. 3492.
23. O.A. Nezhevenko, "On The Limitations of Accelerating Gradient in Linear Colliders Due to the Pulsed Heating," PAC97, Vancouver 1997, p.3013.
24. D.P. Pritzkau, "RF Pulsed Heating," SLAC-Report-577, Ph.D. Dissertation, Stanford University, 2001.
25. J. W. Wang *et al.*, "Recent Progress in R&D of Advanced Room Temperature Accelerator Structures," TH464, LINAC02, Gyeongju, Korea, 2002.
26. V. A. Dolgashev, "Experiments on Gradient Limits for Normal Conducting Accelerators," TU104, LINAC02, Gyeongju, Korea, 2002.
27. V. A. Dolgashev, "High Magnetic Fields in Couplers of X-band Accelerating Structures," TPAB032, PAC03, Portland, Oregon, May 12-16, 2003.
28. Daryl W. Sprehn and Robert E. Kirby of SLAC, private communication.
29. G. A. Mesiats, *Cathode phenomena in a vacuum discharge: the breakdown, the spark and the arc*, Moscow, Nauka Publishers, 2000.

30. V. F. Kovalenko *et al.*, *Thermophysical Processes and Electrovacuum Devices*, Moscow, SOVETSKOE RADIO (1975), pp. 160-193.
31. C. Nantista *et al.*, "Novel Accelerator Structure Couplers," TPAB036, PAC03, Portland, Oregon, May 12-16, 2003.
32. R. J. Loewen *et al.*, "SLAC High Gradient Testing of a KEK X-Band Accelerator Structure," Presented at IEEE PAC99, April 1999, New York, USA.
33. P. B. Wilson, "Gradient Limitation in Accelerating Structures Imposed By Surface Melting,", TPAB039, PAC03, Portland, Oregon, May 12-16, 2003.
34. G. A. Farral, "Voltage Effects of Low and High Current Arcing on Vacuum Interrupter Contacts," *IEEE Trans. on Parts, Hybrids, and Packaging*, Vol. PHP-11, No.2, June 1975.
35. V. V. Shirokov, "Development and Study of High Voltage Accelerating Tubes," PhD. Thesis, Budker INP, Novosibirsk, 1997.
36. A. L. Donaldson and M. Kristiansen, "Utilization of a Thermal Model to Predict Electrode Erosion Parameters of Engineering Importance," IEEE Conference Record of the 1990 Nineteenth Power Modulator Symposium, 26-28 June 1990, pp. 265 -269.
37. A. L. Donaldson, "Electrode Erosion in High-current, High-energy Transient Arcs," Dissertation in Electrical Engineering, Texas Tech University, 1990.
38. J. Haimson and B. Mecklenburg, "A Linear Accelerator Power Amplification System For High Gradient Structure Research," AIP Conf. Proc. **472**, 1003 (1999).